nature cell biology

Homeostatic control of recombination is implemented progressively in mouse meiosis

Francesca Cole[1], Liisa Kauppi[2], Julian Lange[2], Ignasi Roig[2,3], Raymond Wang[1], Scott Keeney[2,4,5] and Maria Jasin[1,5]

Humans suffer from high rates of fetal aneuploidy, often arising from the absence of meiotic crossover recombination between homologous chromosomes[1]. Meiotic recombination is initiated by double-strand breaks (DSBs) generated by the SPO11 transesterase[2]. In yeast and worms, at least one buffering mechanism, crossover homeostasis, maintains crossover numbers despite variation in DSB numbers[3–8]. We show here that mammals exhibit progressive homeostatic control of recombination. In wild-type mouse spermatocytes, focus numbers for early recombination proteins (RAD51, DMC1) were highly variable from cell to cell, whereas foci of the crossover marker MLH1 showed little variability. Furthermore, mice with greater or fewer copies of the *Spo11* gene—with correspondingly greater or fewer numbers of early recombination foci—exhibited relatively invariant crossover numbers. Homeostatic control is enforced during at least two stages, after the formation of early recombination intermediates and later while these intermediates mature towards crossovers. Thus, variability within the mammalian meiotic program is robustly managed by homeostatic mechanisms to control crossover formation, probably to suppress aneuploidy. Meiotic recombination exemplifies how order can be progressively implemented in a self-organizing system despite natural cell-to-cell disparities in the underlying biochemical processes.

Meiotic DSBs initiate a complex cell biological program in which their repair is coupled to chromosome pairing and synapsis, leading to the formation of crossovers. Crossovers physically link homologous chromosomes to ensure accurate segregation at the first meiotic division. DSBs are processed to generate single-stranded DNA onto which the RAD51 and DMC1 proteins load to mediate strand invasion of the homologous chromosome. Pairing and synapsis of homologues ensues while recombination intermediates mature through several steps and DSB repair is completed. Although the control mechanisms are not well understood, each homologue must have at least one crossover (the obligate crossover) and crossovers do not form close to one another (interference)[9]. Recently, in budding yeast and nematodes, crossover homeostasis has been described in which crossover numbers are maintained even with variation in DSB numbers[3,5–8]. This safeguarding of crossovers comes at the expense of non-crossovers[5], an alternative recombination outcome. However, it is unclear what the targets of this homeostatic control are or when during recombination this control is imposed. In mice, as few as 10% of meiotic DSBs are repaired as crossovers and many homologues experience only a single crossover, indicating that progression from DSB formation to maturation of the final crossover product is highly regulated.

To determine whether homeostatic control of meiotic recombination exists in mammals, and if so, when it occurs, we characterized recombination intermediates cytologically in wild-type mouse spermatocytes. RAD51 and DMC1 mark early intermediates, whereas MSH4 localizes to a subset of later, transitional ones, a fraction of which are subsequently marked by MLH1 at mid-pachynema[10,11] (Fig. 1a). These MLH1 foci label ~90% of mammalian crossover sites. Consistent with earlier reports, we observed that numbers of RAD51 and DMC1 foci peak at early zygonema, whereas fewer MSH4 and then MLH1 foci are observed at later prophase stages (Fig. 1b). The decline in recombination focus numbers as meiosis progresses probably reflects sites that have been or will be resolved as non-crossovers, as well as rare sites that will be resolved by MLH1-independent crossover pathways[12].

Cell-to-cell differences in numbers of recombination foci were dynamic, with early foci more variable than later ones. To quantify this pattern, we determined the ratio of the standard deviation to the mean, that is, the coefficient of variation (Fig. 1c). RAD51 and DMC1 foci had large coefficients of variation with overlapping 95% confidence intervals, implying substantial differences between spermatocytes in numbers of recombination intermediates. In contrast, the coefficient of variation was significantly smaller for MSH4 foci and lower still for MLH1, with non-overlapping 95% confidence intervals. Thus, crossover numbers, as measured by MLH1 foci, are relatively constant despite highly variable numbers of early

[1]Developmental Biology Program, Memorial Sloan-Kettering Cancer Center, 1275 York Avenue, New York, New York 10065, USA. [2]Molecular Biology Program, Memorial Sloan-Kettering Cancer Center, 1275 York Avenue, New York, New York 10065, USA. [3]Cytology and Histology Unit, Department of Cell Biology, Physiology, and Immunology, Universitat Autonoma de Barcelona, Barcelona, Spain. [4]Howard Hughes Medical Institute, Memorial Sloan-Kettering Cancer Center, 1275 York Avenue, New York, New York 10065, USA.
[5]Correspondence should be addressed to S.K. or M.J. (e-mail: s-keeney@ski.mskcc.org or m-jasin@ski.mskcc.org)

Received 15 September 2011; accepted 1 February 2012; published online 4 March 2012; DOI: 10.1038/ncb2451

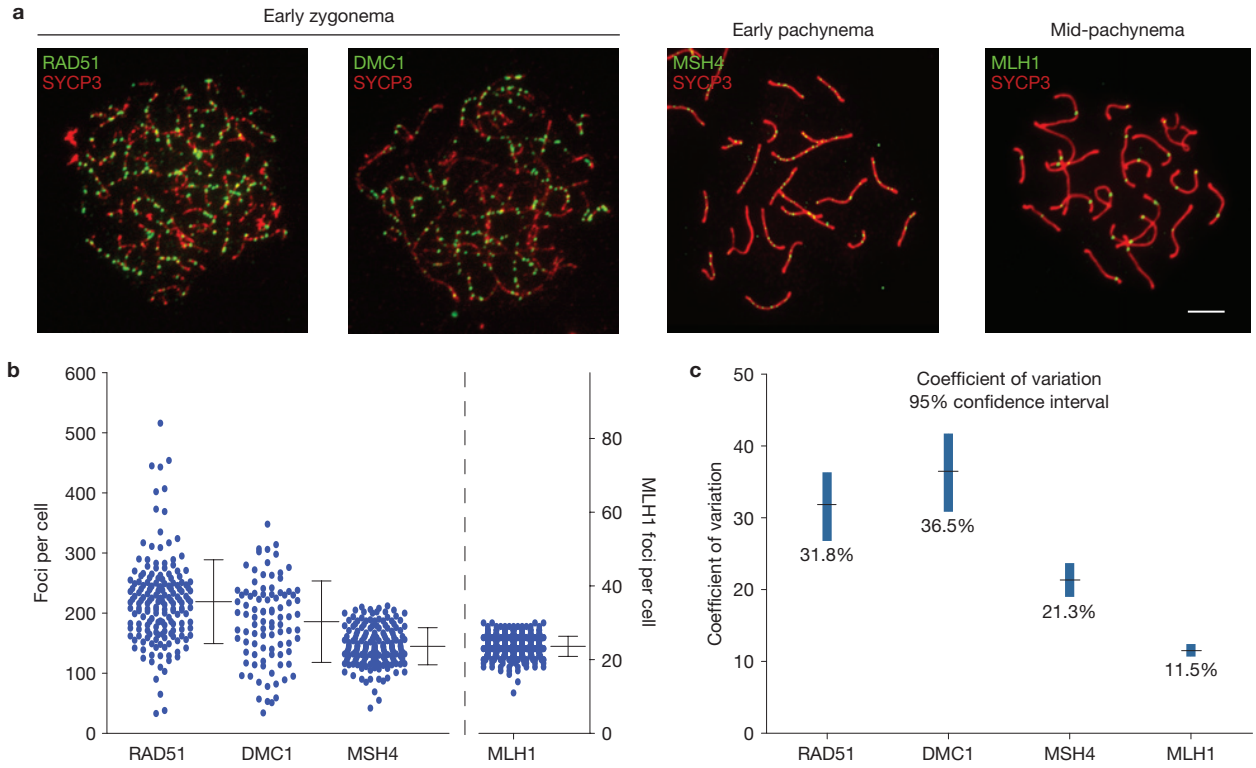

Figure 1 Cell-to-cell variability in numbers of recombination intermediates decreases as meiotic prophase progresses. (**a**) Representative spermatocyte chromosome spreads from various meiosis prophase I stages, stained for the indicated proteins. Scale bar, 5 μm. (**b**) Total foci per nucleus in wild-type spermatocytes. Each dot is the count from a single nucleus. Bars, mean ± s.d. RAD51 and DMC1 at early zygonema (219.2 ± 69.8 and 185.8 ± 67.8, respectively; mean ± s.d.) and MSH4 at late zygonema and early pachynema (144.9 ± 30.9) are plotted on the left axis; MLH1 at mid-pachynema (23.6 ± 2.7) is plotted on the right axis (presented with the mean focus count at the same height as for MSH4, to facilitate comparison). Total mice analysed: RAD51, $n = 8$; DMC1, $n = 5$; MSH4, $n = 4$; MLH1, $n = 9$. (**c**) Coefficients of variation (black line) with 95% confidence intervals (blue line) estimated by bootstrapping (see Methods).

recombination intermediates, indicating that recombination may be homeostatically controlled in mice.

Homeostatic control would imply a cellular response to DSB perturbation[5]. To investigate this, we altered the number of active *Spo11* loci. Wild-type mice (*Spo11*^{wt}) were compared with mice heterozygous for a *Spo11* null allele (*Spo11*^{het}; ref. 13) or overexpressing *Spo11* from a transgene (*Spo11*$^{wt+tg}$), which encodes the SPO11β isoform[14]. SPO11 protein levels corresponded to the genetic locus number: compared with wild-type littermates, *Spo11*^{het} mice expressed roughly half as much of the two main SPO11 isoforms (α and β), whereas *Spo11*$^{wt+tg}$ had approximately twice as much SPO11β (Fig. 2a).

Importantly, the mean number of RAD51 and DMC1 foci also trended with *Spo11* copy number in early meiotic prophase. Compared with *Spo11*^{wt} mice, *Spo11*^{het} mice had ~15% fewer RAD51 foci and ~30% fewer DMC1 foci, whereas *Spo11*$^{wt+tg}$ mice had ~25% more RAD51 and DMC1 foci (Fig. 2b and Table 1). Differences between the *Spo11* genotypes were statistically significant, and all had similarly large coefficients of variation. The first, semi-synchronous wave of meiosis in juveniles yielded results comparable to those in adults (Table 1 and Supplementary Fig. S1). It is notable, however, that the difference in foci between *Spo11*^{wt} versus *Spo11*^{het} or *Spo11*$^{wt+tg}$ mice was less than the expected twofold difference predicted from SPO11 protein levels. We also quantified γH2AX, the phosphorylated form of the histone variant H2AX that is made in response to SPO11-generated DSBs (ref. 15). *Spo11*^{het} mice showed on average about half the level of SPO11-dependent γH2AX when compared with *Spo11*^{wt} mice, and, conversely, *Spo11*$^{wt+tg}$ mice had on average about twice the level of γH2AX when compared with *Spo11*^{wt} littermates (Fig. 2c and Supplementary Fig. S2). Thus, altered *Spo11* copy number resulted in a quantitative change in markers for early recombination intermediates.

Remarkably, mean MLH1 focus numbers were indistinguishable between all three genotypes and showed uniformly small coefficients of variation (Fig. 2d, Table 1 and Supplementary Fig. S1). Moreover, there was no significant difference in the percentage of bivalents lacking an MLH1 focus (data not shown). These results reinforce the conclusion that mouse spermatocytes homeostatically control crossover numbers.

The progressive decrease in the coefficient of variation for recombination foci in wild-type mice (Fig. 1c)—from >30% (RAD51, DMC1) to ~21% (MSH4) to ~11% (MLH1)—indicated that homeostatic control may not be limited to one step in the meiotic recombination pathway. Given that recombination intermediates along the crossover pathway equalize for the different *Spo11* genotypes, we examined whether RAD51 and DMC1 focus counts even out as meiotic prophase progresses and DSBs are repaired. Indeed, we found that all three *Spo11* genotypes had similar mean DMC1 focus numbers by late zygonema (Fig. 3b and Table 1), indicating that at least some degree of recombination homeostasis is implemented by this stage.

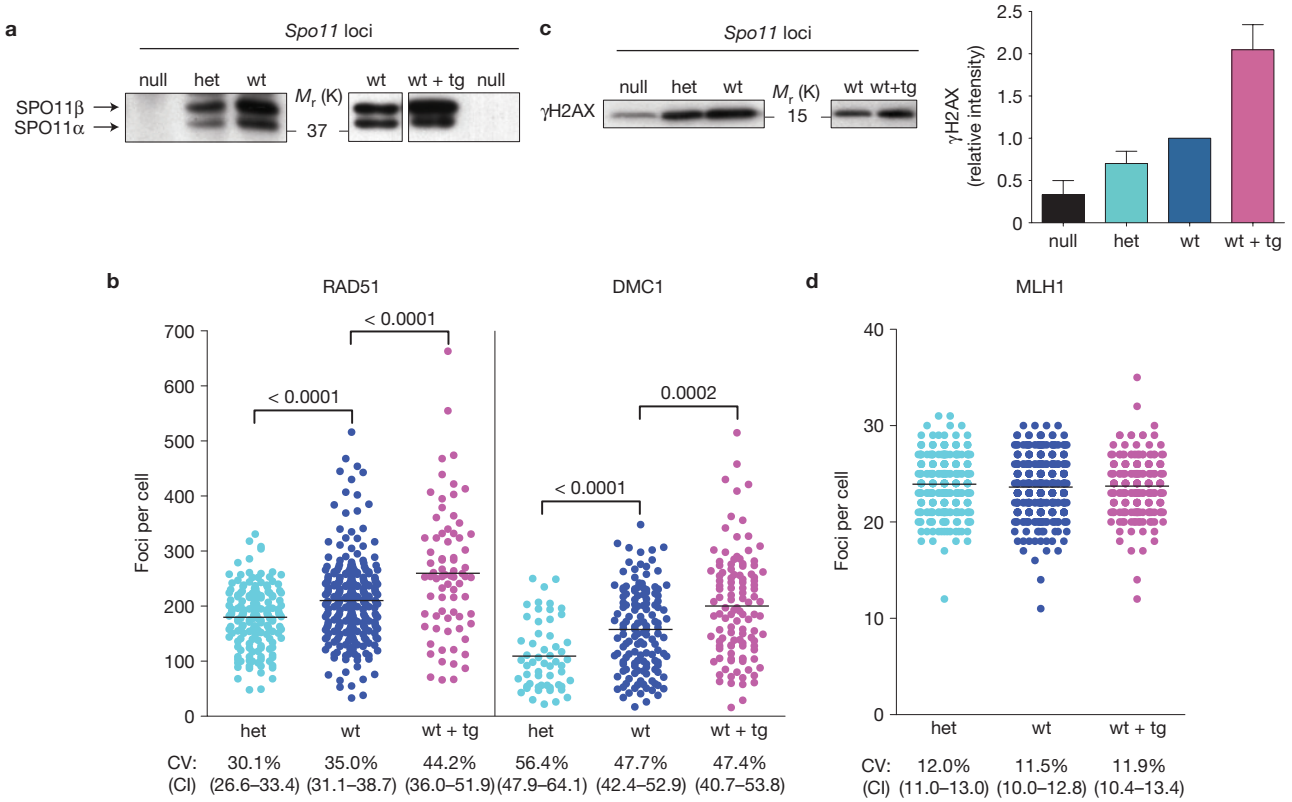

Figure 2 *Spo11* locus number modulates early recombination indicators but not crossover numbers. *Spo11*^{het} and *Spo11*$^{wt+tg}$ mice are fertile and show no obvious meiotic defects, including no difference in the fraction of cells at various stages of meiotic prophase (data not shown). (**a**) Immunoprecipitation followed by western blotting for SPO11 protein. *Spo11* locus composition: *Spo11*^{null} (null), *Spo11*^{het} (het), *Spo11*^{wt} (wt) or *Spo11*$^{wt+tg}$ (wt+tg). The two main isoforms of SPO11 (α and β) are indicated on the left. Coomassie-stained gels were used to verify equivalent amounts of whole-cell extracts from wt and het for immunoprecipitation (see Supplementary Fig. S3a). The transgene expresses only SPO11β (which is known to be proficient for autosomal DSB formation[14]) such that SPO11α serves as a standard for comparison. Representative blots from multiple experiments ($n \geq 4$) are shown. (**b**) RAD51 and DMC1 foci in early meiotic prophase (leptonema and early zygonema, total early in Table 1) per nucleus in spermatocytes with the indicated genotypes. Each circle represents the focus count of a single nucleus. Black bars, means; brackets, *P* values for the indicated comparisons (Mann–Whitney, one-tailed). Mice analysed: RAD51: het, $n=5$; wt, $n=8$; wt+tg, $n=3$; DMC1: het, $n=2$; wt, $n=5$; wt+tg, $n=3$. (**c**) Left, whole-cell extracts from juvenile testes 12 days postpartum (dpp) immunoblotted for γH2AX protein. *Spo11* locus composition is as in **a**. Right, quantification of γH2AX intensity relative to wild type in juvenile testis extracts (mean ± s.d.). Subtracting SPO11-independent γH2AX determined from null mice, hets have on average 55% the level of γH2AX (range ~30–70%) when compared with wt, whereas wt+tg have twice the level (~180–240%). Number of independent mice analysed and ages: null and het versus wt, $n=5$ (11–14 dpp); wt versus wt+tg, $n=3$ (12 dpp). As SPO11-independent γH2AX accompanies formation of the sex body later in meiosis[15], we analysed juvenile males whose testes contain leptotene and zygotene spermatocytes of the first semi-synchronous meiotic wave. (**d**) Autosomal MLH1 focus counts in mid-pachytene spermatocytes. Black bars show the means, which were not statistically significantly different (Mann–Whitney, one-tailed; het versus wt, $P > 0.07$; wt versus wt+tg, $P > 0.3$) Total mice analysed: het, $n=7$; wt, $n=9$; wt+tg, $n=3$. CV, coefficient of variation; CI, 95% confidence interval for the coefficient of variation. Uncropped images of blots are shown in Supplementary Fig. S3.

As with DMC1, mean RAD51 focus numbers also equalized by late zygonema for *Spo11*^{wt} and *Spo11*^{het} spermatocytes (Fig. 3a and Table 1). However, *Spo11*$^{wt+tg}$ mice showed different kinetics of RAD51 foci, with numbers already maximal at leptonema rather than early zygonema and then decreasing but not to the same level as the other genotypes (Fig. 3a). This pattern may reflect precocious and prolonged SPO11β transgenic expression, and hence DSB formation[14]. Consistent with precocious DSB formation, DMC1 focus numbers were also disproportionately high at leptonema in *Spo11*$^{wt+tg}$ mice, even though they eventually equalized with the other genotypes by late zygonema. Possibly, DSBs formed later in meiosis or persistent unrepaired DSBs resulting from transgene expression are shunted to a mitotic-like repair mechanism[16] and are less likely to engage the meiosis-specific DMC1.

The equilibration of DMC1 foci indicates that homeostatic control can be at least partially exerted by late zygonema, but does not address whether it is fully implemented by this stage. To determine whether further homeostatic control is imposed later, as indicated by results from wild-type mice, we examined MSH4 foci, which form coincidentally with DMC1 equilibration. Numbers of MSH4 foci correlated with SPO11 expression: *Spo11*^{het} spermatocytes had 8.4% fewer MSH4 foci than wild type, and *Spo11*$^{wt+tg}$ spermatocytes had 7.0% more (Table 1; $P < 0.0001$ and $P = 0.002$, respectively, one-tailed Mann–Whitney test). As these differences between the genotypes were smaller than for early DMC1 or RAD51 foci, these results are consistent with at least partial implementation of homeostatic control by late zygonema when the number of MSH4 foci is maximal. However, we conclude that a significant fraction of recombination

Table 1 Recombination focus frequencies in different mouse genotypes at different meiotic stages.

		Genotype					
		Spo11^{het}		*Spo11*^{wt}		*Spo11*$^{wt+tg}$	
Marker	**Stage**	**Mean**	**CV**	**Mean**	**CV**	**Mean**	**CV**
RAD51	Leptonema	161.6*	39.8	194.0	40.0	308.2*	43.8
	Early zygonema	190.3*	23.3	219.2	31.8	227.2	38.0
	Late zygonema	130.3	33.0	132.0	44.6	207.6*	38.7
	Early pachynema	n.d.	n.d.	48.2	36.4	85.5*	48.2
	Total early‡	179.9*	30.1	210.1	35.0	259.6*	44.2
	Juvenile	149.9*	37.5	183.8	35.1	n.d.	
DMC1	Leptonema	73.6*	56.2	97.6	53.2	181.2*	54.1
	Early zygonema	129.1*	48.4	185.8	36.5	208.0	44.7
	Late zygonema	120.2	68.4	96.75	55.9	100.4	59.2
	Early pachynema	44.7	59.3	50.1	46.3	58.3	103.6
	Total early‡	109.3*	56.4	157.7	47.7	200.3*	47.4
MSH4	Late zygonema	148.4*	19.7	161.2	19.0	166.6	19.4
	Early pachynema	124.8*	16.2	130.7	17.9	139.9*	14.6
	Total	132.7*	19.6	144.9	21.3	155.1*	19.8
MLH1†	Mid-pachynema	23.9	12.0	23.6	11.5	23.7	11.9
	Juvenile	23.2	12.8	23.6	11.5	n.d.	

Means and coefficient of variation (CV) for each stage, genotype and marker tested. Two to nine independent mice were used for each marker (see figure legends). A similar decrease in RAD51 focus numbers was reported in mice heterozygous for a different *Spo11*-knockout allele[35]. *Significantly different from wild type ($P \leq 0.05$, Mann–Whitney, one-tailed). †Autosome foci alone. ‡Total early combines all focus counts for leptonema and early zygonema nuclei. n.d., not determined.

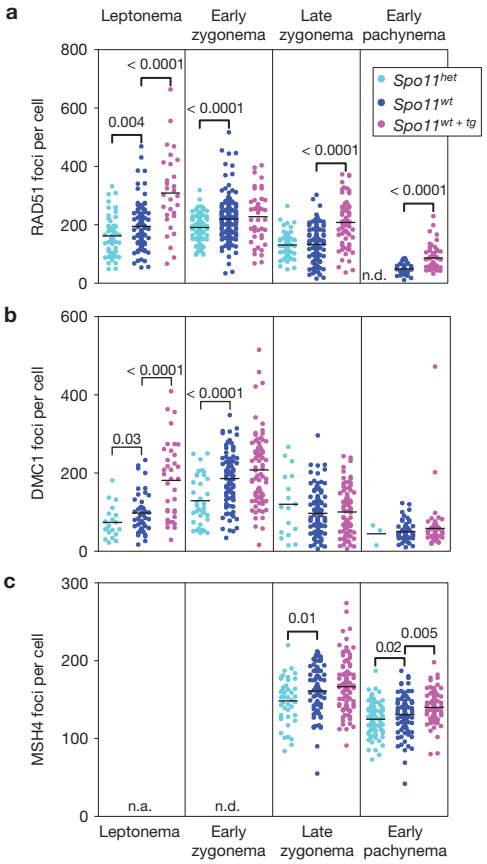

Figure 3 Changes in numbers of recombination-associated foci as meiosis progresses. (**a**) RAD51 foci at the indicated stages. Black bars, means; brackets, statistically significant *P* values (Mann–Whitney, one-tailed). Mice analysed: *Spo11*^{het}, $n = 5$; *Spo11*^{wt}, $n = 8$; *Spo11*$^{wt+tg}$, $n = 3$. (**b**) DMC1 foci. Mice analysed: *Spo11*^{het}, $n = 2$; *Spo11*^{wt}, $n = 5$; *Spo11*$^{wt+tg}$, $n = 3$. (**c**) MSH4 foci. Mice analysed: *Spo11*^{het}, $n = 3$; *Spo11*^{wt}, $n = 5$; *Spo11*$^{wt+tg}$, $n = 3$. n.d., not determined; n.a., not applicable.

intermediates are subject to a homeostatic mechanism later, during pachynema after homologues have fully synapsed: mean MSH4 focus numbers were still different between the *Spo11* genotypes at early pachynema (Fig. 3c), yet MLH1 foci were already equal on first appearance at mid-pachynema. Thus, homeostatic control during meiotic recombination is enforced during at least two stages, after the formation of early recombination intermediates and later while these intermediates mature towards crossovers.

In the view of recombination as a self-organizing process, all manifestations of crossover control are mechanistically related[3,5,9,17]. Homeostasis, interference and obligatory crossover formation are all predicted if the basic logic involves a driving force for crossover designation accompanied by propagation of an inhibitory process along chromosomes that prevents further crossovers from forming nearby[5,17,18]. In contrast, homeostasis and obligatory crossover formation do not follow from deterministic models in which DSBs are fated from the beginning to follow one of two (or more) non-overlapping pathways that generate either interfering or non-interfering crossovers[19]. Progressive implementation of homeostatic control is reminiscent of what is observed for interference, which has also been inferred to occur in at least two stages, at or before MSH4 focus formation and at or before MLH1 focus formation[20]. Hence, recombination homeostasis acts coincidentally with interference. A mechanistic relationship between these phenomena predicts that crossover interference would be similar in the three *Spo11* genotypes. We observed the same degree of interference irrespective of *Spo11* locus number (Fig. 4a,b). As MLH1 foci probably mark all interfering crossovers[11], these results demonstrate that crossover interference is not affected by alterations in numbers of early recombination intermediates, consistent with homeostatic control of recombination and crossover interference arising from a single underlying mechanism[18].

Mammals provide a counterpoint to the two organisms analysed for crossover homeostasis. In yeast, chromosome pairing is dependent on recombination provoked by a large number of DSBs (ref. 21), a

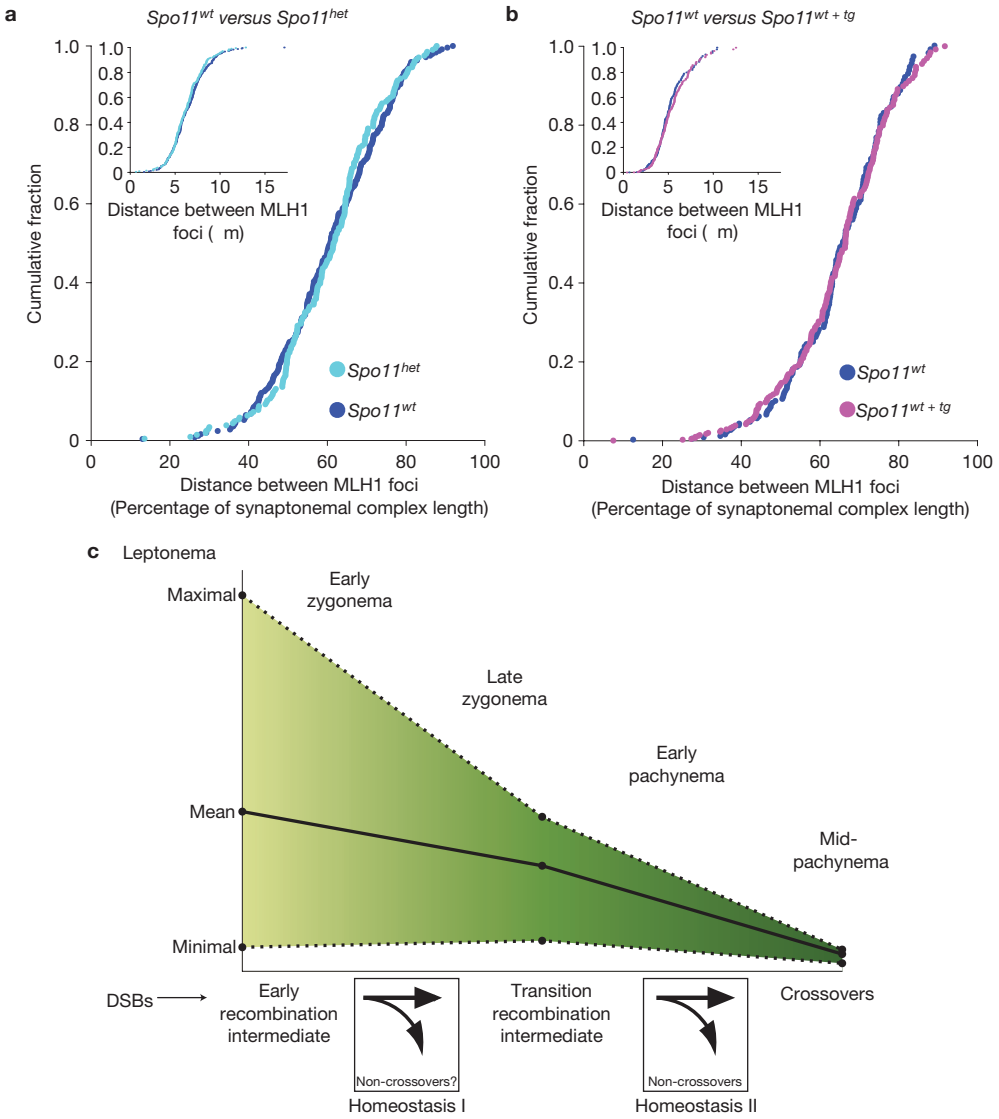

Figure 4 Cytological interference is unchanged despite decreased or increased early recombination intermediates. (**a**) Cytological interference in *Spo11*^{het} versus *Spo11*^{wt} spermatocytes. Distances between MLH1 foci were measured on autosomal bivalents containing ≥ two foci. The cumulative fraction of the inter-focus distances measured as a percentage of synaptonemal complex length or in micrometres (inset) is shown. Number of bivalents analysed: *Spo11*^{het}, $n = 206$; *Spo11*^{wt}, $n = 248$. The *Spo11*^{het} data were previously published[24]. (**b**) Cytological interference in *Spo11*^{wt} versus *Spo11*$^{wt+tg}$ spermatocytes. Number of bivalents analysed: *Spo11*^{wt}, $n = 154$; *Spo11*$^{wt+tg}$, $n = 192$. (**c**) Homeostatic regulation of recombination occurs at two stages. Phases of meiotic prophase are indicated. Black line, wild-type mean focus counts for RAD51 (early recombination intermediate), MSH4 (transition recombination intermediate) and MLH1 (crossovers); dotted line, the maximal and minimal focus count for each marker. A model for progressive homeostatic implementation is depicted below.

large fraction of which (one-half or more) are resolved as crossovers[22]. Interference is relatively weak[3,5,9]. In contrast, worms make many fewer DSBs and these are dispensable for homologous pairing[23]. A smaller but still substantial fraction of DSBs generates crossovers, and both interference and homeostasis are near absolute in this organism[4,8]. Mammals exhibit yet a different combination: pairing requires recombination that is induced by a large number of DSBs (ref. 13; as in yeast), but only a small fraction of DSBs become crossovers (fewer than in worms) and interference is strong but not absolute[20]. The widely different spectra of chromosome behaviour make it difficult to simply extrapolate findings between organisms. In this context, that homeostasis and interference go hand in hand across phyla reinforces the conclusion that they are inextricably linked.

The decreasing variability in numbers of early, transitional and late recombination foci in wild-type mice reported here provides clear evidence that mouse spermatocytes have homeostatic control of recombination, with the end point being exquisite crossover control (Fig. 4c). In principle this control could absorb differences of either absolute DSB number or the kinetics of DSB formation and repair. *Spo11*$^{wt+tg}$ mice almost certainly experience increased absolute DSB numbers, as RAD51 and DMC1 foci at leptonema substantially surpass the counts in *Spo11*^{het} mice at any stage. This result provides evidence for crossover homeostasis. That crossover homeostasis can compensate for increased DSB numbers also provides a new framework to understand previous studies of *Spo11*$^{+/-}$*Atm*$^{-/-}$ spermatocytes, which show only a modest (~10%) increase in the number of

MLH1 foci[24] despite an apparent ~6-fold increase in DSBs (ref. 25). Constant MLH1 focus numbers in the face of increased absolute DSB levels implies that another recombination outcome absorbs the increase, presumably interhomologue non-crossovers as in yeast[3], recombination between sister chromatids[26], non-interfering crossovers as in worms[7,27] or all three. RAD51 focus counts in *Spo11*$^{wt+tg}$ mice support the possibility of a further layer of control with some breaks shunted to a mitotic-like recombination pathway, involving either the juxtaposed homologue or the sister chromatid[16]. In any case, our results indicate that homeostatic control of recombination pathway choice continues even after homologues are fully synapsed.

Removal of a single active copy of *Spo11* (*Spo11*^{het}) may result in fewer DSBs, consistent with crossover homeostasis[5]. As interhomologue non-crossovers represent a substantial portion of DSB repair events in mouse spermatocytes[28], they provide more than adequate 'buffering' capacity to achieve crossover homeostasis. The large ratio of non-crossovers to crossovers limits the ability to discern the small changes in non-crossover numbers expected by altering *Spo11* locus number (Supplementary Table S1). However, an alternative to reduced levels of DSBs is that *Spo11*^{het} mice have modified kinetics of DSB formation and repair. Recent evidence implicates the ATM kinase in regulating SPO11 DSB formation in mouse spermatocytes through a negative feedback loop[25]. In *Spo11*^{het} spermatocytes, early reduced DSB formation might yield less ATM kinase activation and thereby less inhibition of SPO11 DSB activity, ultimately resulting in equivalent DSB numbers to wild type, but with slower kinetics. In support of this interpretation, the concentration of γH2AX, a direct target of the ATM kinase, closely tracked with the number of active *Spo11* loci, whereas numbers of early recombination foci—DSB markers that are further downstream—were less directly proportional to *Spo11* copy number. If correct, this kinetic scenario would describe a different type of homeostasis, namely, control of DSB formation, which might work in conjunction with crossover homeostasis to provide robust, multi-layered control of meiotic recombination.

Recombination initiation by DSB formation is a stochastic process in that each meiotic cell's DSB 'map' is unique, with the location of crossovers (and non-crossovers) differing widely between individuals (for example, refs 3,29). As a result, the breadth of sites engaged in recombination within a population works towards maximizing genetic diversity. We show here that another consequence of this stochasticity is highly variable numbers of DSBs, even among normal mammalian meiocytes. A possible negative outcome is that some cells receive significantly fewer DSBs than the population average, potentially causing chromosome mis-segregation because of failed crossover formation. Homeostatic control, as uncovered here, ensures that crossing over is robust in the face of capricious recombination initiation, enforcing order in the meiotic program despite cell-to-cell variation in the underlying biochemical process.

Consistent with this concept, mouse oocytes are similar to spermatocytes in exhibiting small coefficients of variation for MLH1 focus counts[30,31] and comparably low aneuploidy rates[32]. Human spermatocytes probably have homeostatic mechanisms: from published data (for example, ref. 33), we find that MLH1 focus counts in human spermatocytes have small coefficients of variation, in the same ~10% range as we observed for mouse. In marked contrast, MLH1 foci in human oocytes have a coefficient of variation of >30% (ref. 34), in the range observed for early recombination markers in mouse. Oocytes also mis-segregate chromosomes much more often than spermatocytes in humans[1], raising the question of whether weaker homeostatic mechanisms in human oocytes are a root cause of the high fetal aneuploidy rates experienced by our species. □

METHODS

Methods and any associated references are available in the online version of the paper at www.nature.com/naturecellbiology

Note: Supplementary Information is available on the Nature Cell Biology website

ACKNOWLEDGEMENTS

We thank present and past members of the Jasin and Keeney laboratories for helpful discussions. F.C. was supported by a Ruth L. Kirschstein NRSA (F32HD51392). S.K. is an Investigator of the Howard Hughes Medical Institute. This work was supported by NIH grant HD040916 (to M.J. and S.K.).

AUTHOR CONTRIBUTIONS

F.C., S.K. and M.J. designed the experiments. F.C., L.K., J.L., I.R. and R.W. carried out experiments. F.C., S.K. and M.J. wrote the paper.

COMPETING FINANCIAL INTERESTS

The authors declare no competing financial interests.

Published online at www.nature.com/naturecellbiology
Reprints and permissions information is available online at www.nature.com/reprints

1. Hassold, T., Hall, H. & Hunt, P. The origin of human aneuploidy: where we have been, where we are going. *Hum. Mol. Genet.* **16** (Spec No. 2), R203–R208 (2007).
2. Keeney, S. in *Recombination and Meiosis* (eds Egel, R. & Lankenau, D-H.) 81–123 (Springer, 2007).
3. Chen, S. Y. *et al.* Global analysis of the meiotic crossover landscape. *Dev. Cell* **15,** 401–415 (2008).
4. Hillers, K. J. & Villeneuve, A. M. Chromosome-wide control of meiotic crossing over in *C. elegans*. *Curr. Biol.* **13,** 1641–1647 (2003).
5. Martini, E., Diaz, R. L., Hunter, N. & Keeney, S. Crossover homeostasis in yeast meiosis. *Cell* **126,** 285–295 (2006).
6. Roig, I. & Keeney, S. Probing meiotic recombination decisions. *Dev. Cell* **15,** 331–332 (2008).
7. Youds, J. L. *et al.* RTEL-1 enforces meiotic crossover interference and homeostasis. *Science* **327,** 1254–1258 (2010).
8. Rosu, S., Libuda, D. E. & Villeneuve, A. M. Robust crossover assurance and regulated interhomolog access maintain meiotic crossover number. *Science* **334,** 1286–1289 (2011).
9. Jones, G. H. & Franklin, F. C. Meiotic crossing-over: obligation and interference. *Cell* **126,** 246–248 (2006).
10. Cohen, P. E., Pollack, S. E. & Pollard, J. W. Genetic analysis of chromosome pairing, recombination, and cell cycle control during first meiotic prophase in mammals. *Endocr. Rev.* **27,** 398–426 (2006).
11. Anderson, L. K., Reeves, A., Webb, L. M. & Ashley, T. Distribution of crossing over on mouse synaptonemal complexes using immunofluorescent localization of MLH1 protein. *Genetics* **151,** 1569–1579 (1999).
12. Holloway, J. K., Booth, J., Edelmann, W., McGowan, C. H. & Cohen, P. E. MUS81 generates a subset of MLH1-MLH3-independent crossovers in mammalian meiosis. *PLoS Genet.* **4,** e1000186 (2008).
13. Baudat, F., Manova, K., Yuen, J. P., Jasin, M. & Keeney, S. Chromosome synapsis defects and sexually dimorphic meiotic progression in mice lacking Spo11. *Mol. Cell* **6,** 989–998 (2000).
14. Kauppi, L. *et al.* Distinct properties of the XY pseudoautosomal region crucial for male meiosis. *Science* **331,** 916–920 (2011).
15. Mahadevaiah, S. K. *et al.* Recombinational DNA double-strand breaks in mice precede synapsis. *Nat. Genet.* **27,** 271–276 (2001).
16. Larocque, J. R. & Jasin, M. Mechanisms of recombination between diverged sequences in wild-type and BLM-deficient mouse and human cells. *Mol. Cell Biol.* **30,** 1887–1897 (2010).
17. Zhang, L., Kleckner, N. E., Storlazzi, A. & Kim, K. P. Meiotic double-strand breaks occur once per pair of (sister) chromatids and, via Mec1/ATR and Tel1/ATM, once per quartet of chromatids . *Proc. Natl Acad. Sci. USA* **108,** 20036–20041 (2011).
18. Kleckner, N. *et al.* A mechanical basis for chromosome function. *Proc. Natl Acad. Sci. USA* **101,** 12592–12597 (2004).
19. Stahl, F. W. & Foss, H. M. A two-pathway analysis of meiotic crossing over and gene conversion in *Saccharomyces cerevisiae*. *Genetics* **186,** 515–536 (2010).
20. de Boer, E., Stam, P., Dietrich, A. J., Pastink, A. & Heyting, C. Two levels of interference in mouse meiotic recombination. *Proc. Natl Acad. Sci. USA* **103,** 9607–9612 (2006).

21. Cole, F., Keeney, S. & Jasin, M. Evolutionary conservation of meiotic DSB proteins: more than just Spo11. *Genes Dev.* **24,** 1201–1207 (2010).
22. Mancera, E., Bourgon, R., Brozzi, A., Huber, W. & Steinmetz, L. M. High-resolution mapping of meiotic crossovers and non-crossovers in yeast. *Nature* **454,** 479–485 (2008).
23. Dernburg, A. F. *et al*. Meiotic recombination in *C. elegans* initiates by a conserved mechanism and is dispensable for homologous chromosome synapsis. *Cell* **94,** 387–398 (1998).
24. Barchi, M. *et al*. ATM promotes the obligate XY crossover and both crossover control and chromosome axis integrity on autosomes. *PLoS Genet.* **4,** e1000076 (2008).
25. Lange, J. *et al*. ATM controls meiotic double-strand-break formation. *Nature* **479,** 237–240 (2011).
26. Goldfarb, T. & Lichten, M. Frequent and efficient use of the sister chromatid for DNA double-strand break repair during budding yeast meiosis. *PLoS Biol.* **8,** e1000520 (2010).
27. Mets, D. G. & Meyer, B. J. Condensins regulate meiotic DNA break distribution, thus crossover frequency, by controlling chromosome structure. *Cell* **139,** 73–86 (2009).
28. Cole, F., Keeney, S. & Jasin, M. Comprehensive, fine-scale dissection of homologous recombination outcomes at a hot spot in mouse meiosis. *Mol. Cell* **39,** 700–710 (2010).
29. Coop, G., Wen, X., Ober, C., Pritchard, J. K. & Przeworski, M. High-resolution mapping of crossovers reveals extensive variation in fine-scale recombination patterns among humans. *Science* **319,** 1395–1398 (2008).
30. Baker, S. M. *et al*. Involvement of mouse Mlh1 in DNA mismatch repair and meiotic crossing over. *Nat. Genet.* **13,** 336–342 (1996).
31. de Boer, E., Dietrich, A. J., Hoog, C., Stam, P. & Heyting, C. Meiotic interference among MLH1 foci requires neither an intact axial element structure nor full synapsis. *J. Cell Sci.* **120,** 731–736 (2007).
32. Koehler, K. E., Schrump, S. E., Cherry, J. P., Hassold, T. J. & Hunt, P. A. Near-human aneuploidy levels in female mice with homeologous chromosomes. *Curr. Biol.* **16,** R579–R580 (2006).
33. Ferguson, K. A., Leung, S., Jiang, D. & Ma, S. Distribution of MLH1 foci and inter-focal distances in spermatocytes of infertile men. *Hum. Reprod.* **24,** 1313–1321 (2009).
34. Lenzi, M. L. *et al*. Extreme heterogeneity in the molecular events leading to the establishment of chiasmata during meiosis i in human oocytes. *Am. J. Hum. Genet.* **76,** 112–127 (2005).
35. Bellani, M. A., Boateng, K. A., McLeod, D. & Camerini-Otero, R. D. The expression profile of the major mouse SPO11 isoforms indicates that SPO11β introduces double strand breaks and suggests that SPO11α has an additional role in prophase in both spermatocytes and oocytes. *Mol. Cell Biol.* **30,** 4391–4403 (2010).

METHODS

Mice. All mice used in this study were of the C57BL6/J, 129X1/SvJ or mixed C57BL6/J-129X1/SvJ (Jackson Laboratories) backgrounds. The *Spo11* null allele has been described previously[13] and was genotyped by PCR, as previously described[24]. The $Spo11^{wt+tg}$ (wt + tg) mice are homozygous wild type at the endogenous *Spo11* locus and carry two allelic copies of a previously described $Spo11\beta_B$ transgene[14]. The transgene is expressed by a germ-cell-specific promoter and was genotyped by Southern blotting[14]. All experimental animals were compared with wild-type littermates, with the exception of two $Spo11^{wt+tg}$ animals used for focus counts, which were compared instead with age-matched wild-type (not littermate) animals that were processed in parallel. Numbers of animals analysed for each condition are listed in the figure legends and no significant inter-individual variation was noted. All experiments were carried out in accordance with relevant regulatory standards and were approved by the MSKCC Institutional Animal Care and Use Committee.

Spermatocyte chromosome spreads and immunofluorescence microscopy. Spermatocytes from adult (>8 weeks old) or juvenile (11–13 days postpartum) mice were either surface spread[24] or separated into individual cells in suspension[36] before surface spreading. Immunofluorescence microscopy was carried out as previously described[24]. Antibodies and dilutions used were: SYCP3 (Abcam ab15093 at 1:500 and Santa Cruz sc-74569 at 1:500); RAD51 (EMD PC130 at 1:250); DMC1 (refs 37, 38; Santa Cruz sc-22768 at 1:200); MSH4 (Abcam ab58666 at 1:200); MLH1 (BD Biosciences 51-1327GR at 1:75). After immunostaining, slides were mounted in ProLong Gold antifade reagent with DAPI (Invitrogen). Nuclei were staged by assessing the staining of SYCP3 with these criteria: leptonema, short stretches of axis with no evidence of thickening associated with synapsis; early zygonema, longer cohesive stretches of axis and some synapsis; late zygonema, greater than 50% synapsed axes, but not complete; early pachynema, completely synapsed axes, but less intensely stained sex body chromatin. The genotypes of the samples were blinded until after focus counts were determined. Only axis-associated foci were counted. MLH1 inter-focus distances were assessed as previously described[38].

Immunoprecipitation and western blotting. SPO11 immunoprecipitation and western blots were carried out with adult littermates of the indicated genotypes as previously described for wt versus het[39] and for wt versus wt + tg (refs 14,25). Protein levels between mice were confirmed to be equivalent by BioRad DC protein assay before immunoprecipitation. Quality and relative quantity of extracts were determined by Coomassie staining of whole-cell extracts separated by SDS–PAGE. For γH2AX experiments, decapsulated testes were homogenized by dounce and heated for 10 min at 95 °C in RIPA buffer supplemented with protease (Roche) and phosphatase (Thermo Scientific) inhibitors. Extracts were then cleared by centrifugation. Protein levels in the whole-cell lysate were quantified with the BioRad DC protein assay, equilibrated between littermates and then boiled in 1× Laemmli buffer. Approximately 1/10 of juvenile testis samples was loaded per lane and fractionated by SDS–PAGE (15% gel). Gels were transferred to nylon membranes and western blotted with anti-γ H2AX (Millipore, JBW301) by standard protocols. Equivalent loading was confirmed by quantification of a background band that crossreacts with the anti-γH2AX antibody or by reprobing the blots (without stripping) with an antibody against α-tubulin (Sigma-Aldrich, T9026; Supplementary Fig. S3). Blots were developed with ECL reagent (GE Healthcare) and either directly captured with a Fujifilm Intelligent Dark Box LAS-3000 or exposed to film and scanned in a Kodak Image Station 4000R Pro. Bands of interest were quantified with ImageQuant.

Statistical analysis. The Mann–Whitney test was applied to focus number comparisons to avoid assuming normal distribution. We used a one-tailed test as the expected alteration for reducing ($Spo11^{het}$) or increasing ($Spo11^{wt+tg}$) SPO11 activity is unidirectional. Confidence intervals of coefficients of variation were estimated by bootstrap resampling (10,000 replicates, percentile method) using the 'boot' package in R (version 2.13.1; http://cran.r-project.org).

Crossovers and non-crossovers at the *A3* hotspot in $Spo11^{wt}$ and $Spo11^{het}$ mice were determined as previously described using C57BL6/J x DBA/2J F1 hybrid mice[28] (Supplementary Table S1). On the basis of the ratio of crossovers to non-crossovers, a power analysis[40] was carried out to determine the total number of recombinants required per genotype to ensure an 80% chance of observing a statistically significant result.

36. Heyting, C. & Dietrich, A. J. Meiotic chromosome preparation and protein labeling. *Methods Cell Biol.* **35,** 177–202 (1991).
37. Dray, E. *et al.* Molecular basis for enhancement of the meiotic DMC1 recombinase by RAD51 associated protein 1 (RAD51AP1). *Proc. Natl Acad. Sci. USA* **108,** 3560–3565 (2011).
38. Roig, I. *et al.* Mouse TRIP13/PCH2 is required for recombination and normal higher-order chromosome structure during meiosis. *PLoS Genet.* **6,** e1001062 (2010).
39. Neale, M. J., Pan, J. & Keeney, S. Endonucleolytic processing of covalent protein-linked DNA double-strand breaks. *Nature* **436,** 1053–1057 (2005).
40. Cohen, J. *Statistical Power Analysis for the Behavioral Sciences* 2nd edn (Lawrence Erlbaum Associates, Inc., 1988).

DOI: 10.1038/ncb2451

nature cell biology

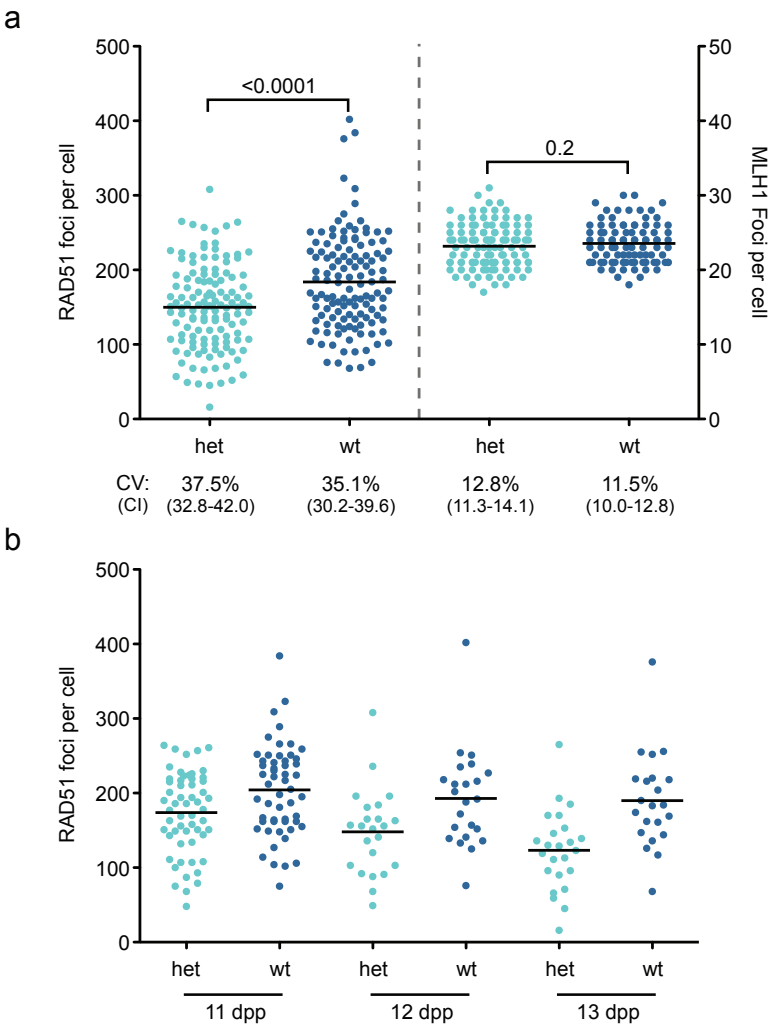

Figure S1 Recombination homeostasis in the semi-synchronous meiosis of juvenile males. **a)** Total foci per nucleus are shown for RAD51 at leptonema and early zygonema (left axis, 11 – 13 dpp) or MLH1 at mid-pachynema (right axis, 21, 22 and 33 dpp) between *Spo11*^{het} and *Spo11*^{wt} juvenile littermates. **b)** Time course of leptonema and early zygonema RAD51 focus counts. Bars, means; brackets, p values (Mann-Whitney, one-tailed). Mice analyzed for RAD51: *Spo11*^{het}, n = 6; *Spo11*^{wt}, n = 6 (11 dpp, n = 2; 12 dpp, n = 3; 13 dpp, n = 1) and MLH1: *Spo11*^{het}, n = 3; *Spo11*^{wt}, n = 3.

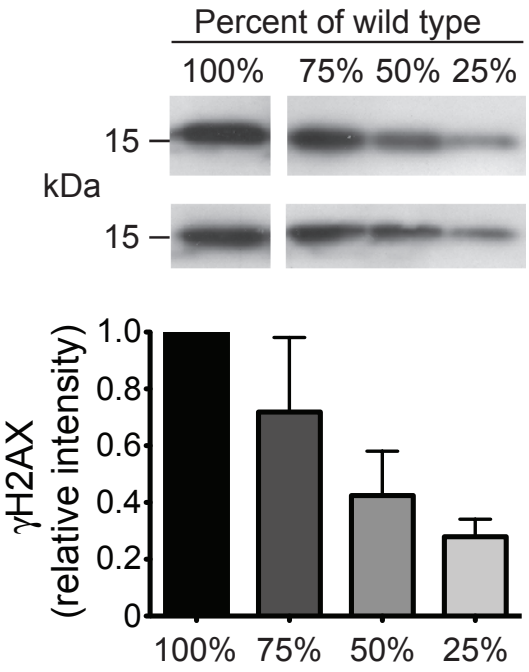

Figure S2 Titration curve for γH2AX immunoblotting. Above, two examples of γH2AX immunoblots for 13 (top) and 12 (middle) dpp whole testis extracts. Varying equivalents from a wild-type sample were loaded in each lane, as indicated. The positions of molecular weight markers (kDa) are shown. Below, quantification of four independent experiments for γH2AX intensity relative to the 100% equivalent sample. Error bars, SD.

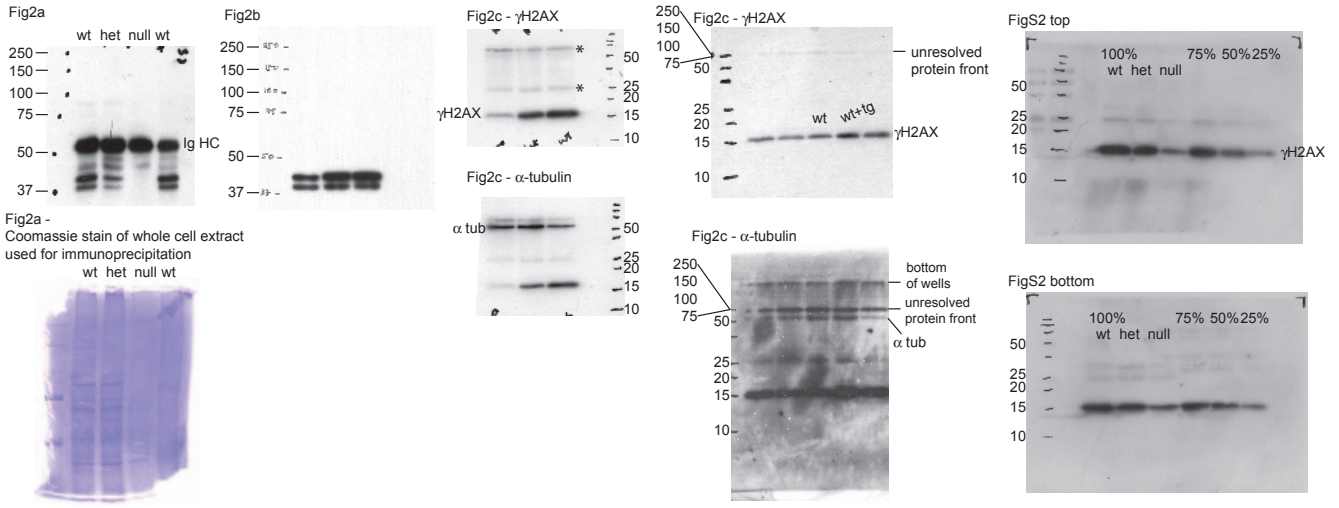

Figure S3 Uncropped gel scans. Corresponding to Fig. 2a: Coomassie-stained gel of whole cell extracts from testes used for SPO11 immunoprecipitation is shown below the whole gel scan of the western blot. Corresponding to Fig. 2c: Left, Asterisks in the γH2AX western blot indicate background bands that cross-react with the anti-γH2AX antibody which were used to confirm equivalent loading.

Table S1: Recombination analysis from different mouse genotypes.

Spo11	Crossovers	Noncrossovers	Total	P value	Total required
wt	18	94	112		1694
het	17	71	88	0.3387	1694

The number of crossovers and noncrossovers at the *A3* hotspot were determined from $Spo11^{wt}$ and $Spo11^{het}$ littermates (n=2 mice; 10,720 and 9,200 sperm genomes screened in $Spo11^{wt}$ and $Spo11^{het}$, respectively). We observed a ~20% reduction in noncrossovers relative to crossovers in $Spo11^{het}$ compared to $Spo11^{wt}$. This reduction approximates that predicted from cytological analysis of recombination foci, although as indicated, the difference is not statistically significant (Fisher's exact test, one-tailed). We performed a power analysis based on these data to determine the total number of recombinants required per genotype to ensure an 80% chance of observing a statistically significant result (Total required). Analyzing such large numbers of recombinants, in particular the more difficult to score noncrossovers, is not experimentally feasible with current technologies.